

Text-guided Eyeglasses Manipulation with Spatial Constraints

Jiacheng Wang, Ping Liu*, Jingen Liu, Wei Xu*,

Abstract—Virtual try-on of eyeglasses involves placing eyeglasses of different shapes and styles onto a face image without physically trying them on. While existing methods have shown impressive results, the variety of eyeglasses styles is limited and the interactions are not always intuitive or efficient. To address these limitations, we propose a Text-guided Eyeglasses Manipulation method that allows for control of the eyeglasses shape and style based on a binary mask and text, respectively. Specifically, we introduce a mask encoder to extract mask conditions and a modulation module that enables simultaneous injection of text and mask conditions. This design allows for fine-grained control of the eyeglasses’ appearance based on both textual descriptions and spatial constraints. Our approach includes a disentangled mapper and a decoupling strategy that preserves irrelevant areas, resulting in better local editing. We employ a two-stage training scheme to handle the different convergence speeds of the various modality conditions, successfully controlling both the shape and style of eyeglasses. Extensive comparison experiments and ablation analyses demonstrate the effectiveness of our approach in achieving diverse eyeglasses styles while preserving irrelevant areas.

Index Terms—Eyeglasses virtual try-on, Text-guided face attributes manipulation, Generative adversarial network.

I. INTRODUCTION

VIRTUAL try-on technology allows individuals to virtually add fashion items to their personal images, facilitating the assessment of suitability and appeal. Specifically, virtual try-on for eyeglasses enables users to try on a variety of styles without physical presence. This approach is highly efficient and convenient, as it eliminates the need for individuals to physically try on numerous eyeglasses to determine the appropriate style and shape. Moreover, virtual try-on technology for eyeglasses has gained popularity due to the emergence of short videos, as it enables users to apply various styles to recorded videos for enhanced visual effects, commonly referred to as “eyeglasses special effects” in different applications.

Several approaches have been proposed to improve eyeglasses virtual try-on technology [1]–[8]. These approaches can be broadly classified into two categories: 3D-based and 2D-based methods. 3D-based methods [1]–[5] employ 3D

J. Wang and W. Xu are with the Hubei Key Laboratory of Smart Internet Technology, School of Electronic Information and Communications, Huazhong University of Science and Technology, Wuhan 430074, China, e-mail: jiacheng@hust.edu.cn, xuwei@hust.edu.cn.

P. Liu is with the Center for Frontier AI Research (CFAR), Research Agency for Science, Technology and Research (A*STAR), Singapore 138634, e-mail: pino.pingliu@gmail.com.

J. Liu is with Disney Streaming Advanced Research, USA, email: jingen.liu@gmail.com.

* means co-corresponding author.

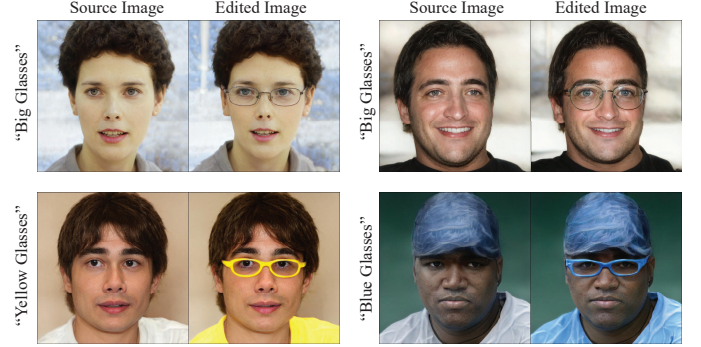


Fig. 1. Issues existing on text-guided virtual try-on for eyeglasses. The first row depicts that eyeglasses in the editing results are of different sizes based on the same text prompt of “big glasses”. The second row shows an entangled phenomenon that irrelevant areas are significantly modified, especially in the cloth region.

eyeglasses models to align the eyeglasses with the face. In contrast, 2D-based methods [6]–[8] directly edit input images using generative adversarial networks (GANs) [9] to produce the desired eyeglasses, which generally rely on the learned latent space to perform eyeglasses manipulation. However, a limitation of these methods is that the introduction of new eyeglasses styles typically requires either building new 3D eyeglasses models [1], [2] for 3D-based methods or recalculation of editing directions in the latent space [7], [8] for 2D-based methods. This can be inefficient and inconvenient to scale.

Constructing new 3D eyeglasses models or recalculating editing directions in the latent space can be a cumbersome task, potentially hindering the speed of adding more diverse eyeglasses styles. One alternative solution to this issue is to leverage text input as a means of conveniently scaling diverse eyeglasses styles. For example, generating sunglasses in an original image based on a simple text prompt of “sunglasses” is a straightforward and intuitive process. Vision-Language models, such as Contrastive Language-Image Pre-training (CLIP) [10], have enabled various methods for arbitrary text-guided image manipulation [11]–[14]. StyleCLIP [11], in particular, is a pioneering work in this area, leveraging the powerful text-to-image alignment capabilities of CLIP [10] to manipulate original images based on text descriptions. The loss supervision technique proposed in StyleCLIP [11] enables the desired eyeglasses style that matches a given text description to be achieved.

Although StyleCLIP provides a more convenient and intuitive way to control eyeglasses than other 2D-based methods [7], [8], it can be difficult to express the degree of editing

precisely, particularly for the spatial configuration (*e.g.*, sizes, shapes) of eyeglasses, which is critical for eyeglasses virtual try-on. For instance, using the same text prompt of “big glasses” may produce different editing results with eyeglasses of varying sizes, as illustrated in Fig. 1. Furthermore, due to the ambiguity and subjectivity of natural language [15], size words such as “small”, “medium”, and “large” may not be consistent with the absolute pixel sizes of items in images, making it unsuitable to control the shape of eyeglasses based solely on simple text prompts.

To accurately control the spatial configuration of eyeglasses without adding excessive complexity to the interaction process, prior knowledge can be introduced, such as landmarks [16], semantic segmentation maps [17], or binary masks [18]. However, facial landmark detection algorithms [19], [20] that detect contour points of eyeglasses are not commonly available, which makes it challenging to automatically collect eyeglasses landmarks and construct sufficient data pairs. Additionally, using semantic segmentation maps [17], [21], [22] that contain complete facial segmentation information may be redundant for controlling the shape of eyeglasses, and requiring users to provide a complete facial segmentation map during the interaction process would increase the workload.

To address these challenges, we designed a text-guided eyeglass manipulation method with spatial constraints. Inspired by HairCLIP [12], we harness the remarkable capacity for expression in textual descriptions to manipulate diverse styles of eyeglasses using a single model. However, different from HairCLIP, our approach integrates spatial constraints through the use of eyeglasses masks. Specifically, the mask is generated by an off-the-shelf face parser on the FFHQ [23] and CelebA-HQ [24] datasets, which are then used to construct aligned data pairs based on the original face pose. Introducing spatial constraints enables better control of the spatial configuration of eyeglasses, without adding excessive complexity to the interaction process. Compared to HairCLIP, there are several crucial modifications:

Firstly, we introduce a mask encoder comprising multiple convolutional blocks to extract mask conditions, which are then employed to control the spatial configuration of eyeglasses for more precise manipulation. Simultaneously, we design a modulation module to allow for the simultaneous injection of text and mask conditions. Utilizing the binary eyeglasses mask and straightforward text prompts, we can effortlessly regulate the shape and style of eyeglasses within a single model.

Secondly, as shown in Fig. 1, modifying the eyeglasses region conditioned on text prompts often leads to noticeable changes in unrelated areas, such as the clothing region, which is a common entangled phenomenon in existing methods. To address the entangled issue, we propose GlassMapper, which consists of an editing mapper and a disentangled mapper to enable more distinct and disentangled editing directions. The editing mapper is responsible for controlling the eyeglasses style, while the disentangled mapper preserves irrelevant areas. We achieve this by employing a simple yet effective decoupling strategy, which involves truncating the gradient flow from the disentangled mapper to the editing mapper.

Thirdly, we adopt a two-stage training scheme to simultaneously control the style and shape of eyeglasses based on different modality conditions. We sequentially equip the GlassMapper with the ability to modify eyeglasses. We conduct comprehensive experiments to demonstrate the improved capability of our approach in achieving diverse eyeglasses styles without modifying irrelevant regions.

In summary, our contributions are as follows:

- We propose a Text-guided Eyeglasses Manipulation method to achieve diverse and flexible eyeglasses virtual try-on. Our method controls eyeglasses shape and style based on a simple binary eyeglasses mask and text description, respectively. This approach accommodates a wide range of eyeglasses shapes and common styles within a single model, offering a more convenient and intuitive mode of interaction.
- To support multiple modalities of information in a single model, we propose a new modulation module that combines the binary eyeglasses mask and natural language descriptions. Furthermore, we employ a two-stage training scheme to stabilize the training process, sequentially equipping our method with the ability to modify eyeglasses.
- To better preserve irrelevant areas, we introduce a disentangled mapper and a simple decoupling strategy, resulting in better local editing. This allows for more accurate and precise control over the eyeglasses style and shape, while also maintaining the integrity of the surrounding areas in the image.
- Extensive quantitative and qualitative experiments on the CelebA-HQ dataset [24] are conducted to demonstrate the superiority of our approach. On average, we outperform the state of the arts [25] by 9.21%, 29.32%, and 11.13% on *Structure Similarity Index Measure* (SSIM) [26], *Peak Signal to Noise Ratio* (PSNR) [27], and *Identity Discrepancy Scores* (IDS), respectively.

II. RELATED WORK

A. Eyeglasses virtual try-on

The goal of eyeglasses virtual try-on is to add eyeglasses with a specific style to the face of an image or video, which is opposite to eyeglasses removal [28], [29]. This can be accomplished through two main categories of methods: 3D-based eyeglasses virtual try-on and 2D-based eyeglasses virtual try-on. 3D-based eyeglasses virtual try-on methods [1]–[5] typically add eyeglasses to a face image by aligning the 3D models of eyeglasses and face. For example, Milanova et al. [1] proposed a markerless eyeglasses virtual try-on system that overlays the 3D eyeglasses model over the face image according to the estimated head pose. Similarly, Feng et al. [2] achieved 3D eyeglasses virtual try-on by combining 3D face reconstruction and pose estimation techniques. They first rotate the 3D eyeglasses model to match the head pose and then put the aligned virtual eyeglasses on the reconstructed 3D face model. While there are many real-time eyeglasses virtual try-on systems based on 3D models, each change of

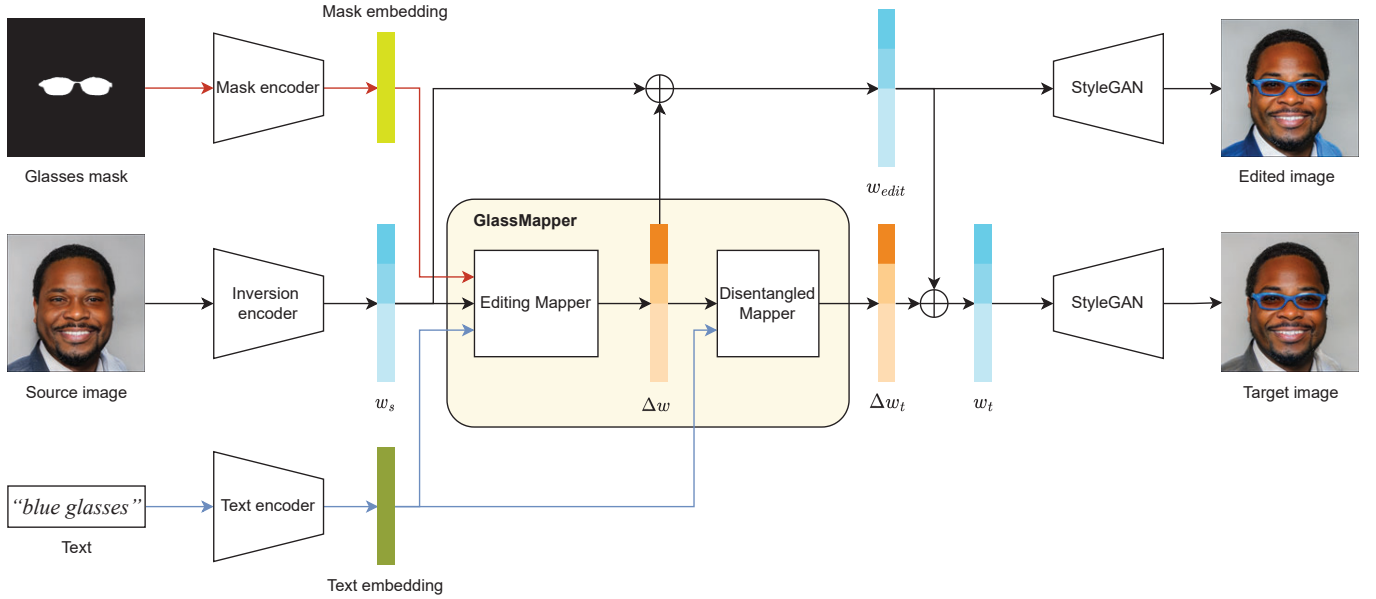


Fig. 2. The overview of our framework. Our framework takes as input the source latent code w_s , which is passed through GlassMapper to predict a disentangled editing direction based on the mask condition e_m and text condition e_t . The details of GlassMapper are provided in Section III-C. The resulting editing direction is applied to the target image, resulting in generated eyeglasses that are well-aligned with the given mask and text conditions. Specifically, the generated eyeglasses match the mask’s shape, and their style corresponds to the text description.

eyeglasses style requires a new 3D eyeglasses model, which can be difficult to collect and scale.

2D-based eyeglasses virtual try-on methods [6]–[8], [30], [31] directly edit the given images to obtain the desired eyeglasses. Some methods [7], [8], [30] use pre-trained GANs, specifically StyleGAN [23], [32], and learn an editing direction in their latent space to control the generated eyeglasses style. Others [6], [31] mainly train an encoder and a generator from scratch, where the encoder extracts the latent representation of the original image and the generator achieves arbitrary eyeglasses style manipulation based on different attribute constraints. However, the variations of generated eyeglasses in these methods are limited, *e.g.*, only black plastic eyeglasses or sunglasses can be added in most cases. To handle this limitation, a concurrent work GlassGAN [33] focuses on multi-style eyeglasses virtual try-on using pre-trained StyleGAN [23], [32]. They explore the editing directions targeted toward eyeglasses in an unsupervised setting, *i.e.*, solving an eigen-problem. However, they need to subjectively assign human-interpretable attributes to the explored editing directions, such as size, position, squareness, roundness, cat-eye appearance, and thickness, which are limited to express the spatial consistency of generated eyeglasses.

B. Text-guided image manipulation

Facial image manipulation [34]–[38] endeavors to alter facial attributes in accordance with user predilections, including images [36], [38], sketches [34], and textual descriptions [35]. In pursuit of a more convenient and intuitive means of manipulation interaction, text-guided image manipulation aims to modify source images according to simple text descriptions, while preserving irrelevant areas. CLIP [10] is a vision-language model trained on 400 million text-image pairs that

can be used to evaluate the similarity between images and texts. With the powerful capabilities of CLIP, StyleCLIP [11] proposed a CLIP loss to make the editing results consistent with the given text. Later, to better preserve irrelevant areas and learn a more disentangled editing direction, several works [25], [39] proposed disentangled loss functions, and [40] learned an attention mask to limit editing areas. Given that the original CLIP loss proposed in StyleCLIP is vulnerable to adversarial samples, [13], [14], [41] modified the CLIP loss using data augmentation or contrastive learning to improve robustness.

Several works [42]–[45] achieved arbitrary text-guided image manipulation without inference-time optimization or restricting to single attribute editing. Specifically, [42]–[44] focused on bridging the latent space of StyleGAN [23], [32] and CLIP [10], while [45] injected text conditions into an attention decoder to obtain corresponding editing directions. With the development of diffusion models, several works [46]–[48] combined CLIP with diffusion models [49]–[51] to handle the limitations of GAN inversion [46] and extend the image manipulation domain [47], [48]. HairCLIP [12] is another recent work that focuses on the diversity of specific attributes, specifically hair attributes, which achieves control of 44 hairstyles and 12 hair colors simultaneously.

In this study, we employ straightforward textual cues to control the eyeglasses style for a more user-friendly and intuitive interface. Furthermore, to precisely regulate the spatial configuration of the eyeglasses without introducing undue intricacy, we suggest the implementation of a binary eyeglasses mask as a spatial constraint. Our framework is inspired by HairCLIP [12] and incorporates several significant modifications to adapt to the task of eyeglasses virtual try-on. Firstly, we modify the modulation module in HairCLIP to adapt to the additional

mask conditions, which allows us to control the size and shape of eyeglasses. Secondly, we introduce a disentangled mapper to preserve the irrelevant areas without compromising the diversity and realism of the generated eyeglasses. In this way, we achieve flexible and diverse eyeglasses virtual try-on in a convenient interaction process, requiring only masks and text as input, which are easy to access. Our framework allows users to easily try on different eyeglasses styles and shapes, making the process of choosing eyeglasses more efficient and convenient.

III. METHOD

A. Overview

Given a mask that shows the shape of eyeglasses, and a text describing the style of eyeglasses, we aim to generate eyeglasses with desired shape and style conditioned on the given mask and text. Therefore, we propose a Text-guided Eyeglasses Manipulation method to control both the shape and style of eyeglasses, which comprises three information encoders, a GlassMapper, and a pre-trained StyleGAN [23], [32] generator. To preserve irrelevant areas without compromising the realism of generated eyeglasses, we propose a decoupling strategy that equips the GlassMapper with abilities to achieve diverse eyeglasses styles and preserve irrelevant areas. Moreover, to control eyeglasses styles and shapes based on different modality conditions simultaneously, we also utilize a two-stage training scheme that is pivotal for stabilizing the training process.

We first present a succinct overview of the fundamental concepts of StyleGAN and CLIP in Section III-B. Subsequently, in Section III-C, we will provide a comprehensive examination of our proposed framework, including the conditional information encoder, the GlassMapper, and the decoupling strategy. Section III-D will contain a thorough examination of the loss functions implemented during the training process. Finally, in Section III-E, we will present the two-stage training scheme and its corresponding objective functions.

B. Preliminary

1) *StyleGAN*: StyleGAN [23], [32] is a generative model that is capable of synthesizing high-resolution and high-fidelity images in a progressive manner. It originates from a learned constant input and modulates the “style” of the image at each convolution layer based on the latent code, thereby directly manipulating the magnitude of image features at different scales. During the synthesis process, there are several latent spaces where we can manipulate the latent code to achieve desired changes to the corresponding image. The original latent space, $\mathcal{Z} \in \mathbb{R}^{512}$, is sampled from a standard Gaussian distribution. Random noise $z \in \mathcal{Z}$ is then transformed into $\mathcal{W} \in \mathbb{R}^{512}$ by a mapping network that consists of 8 fully connected layers. Several studies [7], [8] have demonstrated the good semantic decoupling properties of the \mathcal{W} space and achieved controllable image manipulation by modifying $w \in \mathcal{W}$. The latent code $w \in \mathcal{W}$ is further transformed into StyleSpace \mathcal{S} [52] using a learned affine transformation, where each style parameter s controls an intermediate feature

map. To improve reconstruction performance, the \mathcal{W} space is expanded to $\mathcal{W}+$ space [53]. It has been shown [54] that the reconstruction ability of $\mathcal{W}+$ space is better than that of \mathcal{W} space, while the editability is slightly lower.

2) *CLIP*: The CLIP model comprises an image encoder and a text encoder, which encode images and text into $e_i \in \mathbb{R}^{512}$ and $e_t \in \mathbb{R}^{512}$, respectively. By utilizing a contrastive learning framework and minimizing the cosine distance between positive text-image pairs, CLIP learns a powerful multi-modal embedding space, where we can measure the similarity between text and images. For text-guided image manipulation tasks, StyleCLIP [11] calculates a similarity score between the manipulated image and the target text and then guides the manipulation by maximizing this similarity score, which is formulated by a Global CLIP loss:

$$\mathcal{L}_{\text{global}} = 1 - \cos(E_I(I_{\text{edit}}), E_T(t_{\text{tar}})), \quad (1)$$

where $E_T()$ and $E_I()$ denote the text encoder and image encoder of CLIP, respectively, I_{edit} is the manipulated image, t_{tar} is the target text, $\cos()$ is cosine similarity.

However, as noted in [14], the Global CLIP loss is vulnerable to adversarial examples where small pixel-level perturbations may result in a significant difference in CLIP loss. To address this, they propose another loss function, the Directional CLIP loss, which aligns the directions between the source and target text-image pairs. It is formulated as follows:

$$\begin{aligned} \mathcal{L}_{\text{dir}} &= 1 - \frac{\Delta I \cdot \Delta T}{|\Delta I| \cdot |\Delta T|}, \\ \Delta T &= E_T(t_{\text{tar}}) - E_T(t_{\text{src}}), \\ \Delta I &= E_I(I_{\text{edit}}) - E_I(I_{\text{src}}), \end{aligned} \quad (2)$$

where I_{src} is the source image, t_{src} is the source text which is typically a neutral description such as “a face”.

C. Framework

In our approach, we are inspired by previous works such as StyleCLIP [11] and HairCLIP [12] and utilize a pre-trained StyleGAN to generate high-quality face images. As the $\mathcal{W}+$ space has good semantic decoupling properties, we leverage it to learn a GlassMapper that predicts editing directions based on the mask and text conditions to control the shape and style of eyeglasses.

To generate the editing image, we start by obtaining the source latent code $w_s \in \mathcal{W}+$, the mask condition e_m , and the text embedding e_t through a StyleGAN inversion model, a mask encoder, and a CLIP text encoder, respectively, given a real image I_{src} , a eyeglasses mask m , and a text description t .

The obtained information is then sent to the GlassMapper, which consists of an editing mapper and a disentangled mapper. The editing mapper predicts an editing direction Δw based on e_m and e_t while the disentangled mapper predicts a more decoupling editing direction Δw_t based on e_t , given the calculated editing direction Δw . Finally, the target latent code $w_t = w_{\text{edit}} + \Delta w_t$ is fed into StyleGAN to generate the final editing image I_{tar} .

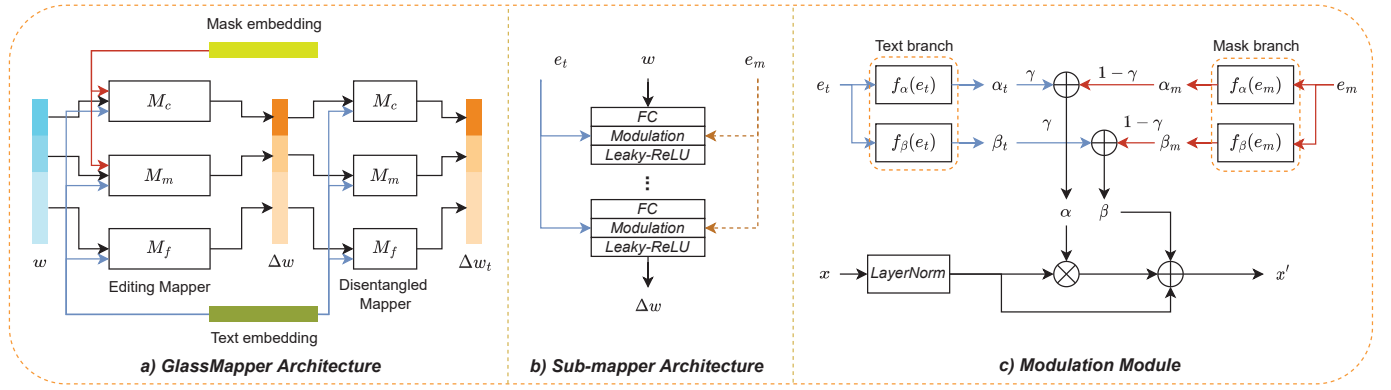


Fig. 3. The architecture of GlassMapper. a) GlassMapper is composed of an editing mapper and a disentangled mapper, each of which is divided into three sub-mappers. b) Each sub-mapper consists of 5 blocks, which are stacked with a fully connected layer, a modulation module, and a leaky ReLU activation layer. c) The modulation module is responsible for modulating the input $x \in \mathbb{R}^{512}$ based on the mask condition $e_m \in \mathbb{R}^{512}$ and text condition $e_t \in \mathbb{R}^{512}$.

Conditional Information Encoder: For text descriptions, a pre-trained CLIP [10] text encoder is used to extract an expressive text embedding $e_t \in \mathbb{R}^{512}$. However, for eyeglasses masks, there is no pre-trained eyeglasses mask encoder available. Therefore, a convolutional neural network, similar to that used in MaskGAN [17], is employed to extract mask conditions. The mask encoder consists of 5 convolutional blocks, each comprising a convolutional layer, an instance normalization layer, and a ReLU activation layer. Given an eyeglasses mask, the mask encoder extracts the corresponding mask embedding $e_m \in \mathbb{R}^{512}$. These mask and text embeddings are then used to condition the GlassMapper and control the shape and style of eyeglasses in the manipulated image I_{edit} .

GlassMapper Architecture: In Fig. 3, we can see that GlassMapper comprises of two mappers: editing mapper and disentangled mapper. Studies [11], [55] have demonstrated that different layers of StyleGAN control different levels of semantic information in the generated image. For instance, shallow layers control coarse-grained information like head pose and facial expressions, while deep layers control fine-grained information like color and micro details. Therefore, we divide the editing mapper into three sub-mappers, namely M_c , M_m , and M_f , each controlling different semantic levels in the generated image. M_c and M_m are responsible for controlling coarse-grained information like eyeglasses shape, while M_f controls fine-grained information such as eyeglasses color. Similar to HairCLIP [12], each sub-mapper consists of 5 blocks, and each block consists of a fully connected layer, a modulation module, and a leaky relu activation layer, as shown in Fig. 3. We split the source latent code w_s into three parts: w_c , w_m , and w_f , which represent different semantic information. Since we want to control eyeglasses shape based on the mask, we inject the mask conditions into M_c and M_m . On the other hand, we use text to control eyeglasses style, which involves fine-grained information like eyeglasses color, so we inject text conditions into all sub-glasses mappers. Therefore, the editing mapper can be expressed as:

$$\begin{aligned} M(w_s, e_t, e_m) \\ = (M_c(w_c, e_t, e_m), M_m(w_m, e_t, e_m), M_f(w_f, e_t)). \end{aligned} \quad (3)$$

Though we succeed to generate eyeglasses with diverse

shapes and styles through the editing mapper, there is still an entangled phenomenon that irrelevant areas are significantly modified, especially in the cloth region. Therefore, we introduce a disentangled mapper to preserve the irrelevant areas without compromising the correctness and realism of the generated eyeglasses.

Disentangled mapper is similar to the editing mapper but with two differences: 1) The number of blocks is set to 2, less than the editing mapper, according to a simpler goal that reduces the modification in the irrelevant areas; 2) Considering that large modifications in the irrelevant areas are always accompanied by the change of eyeglasses style, we only keep the text branch in the modulation module, ensuring the capability of dealing with different text descriptions. Therefore, the disentangled mapper can be expressed as:

$$\begin{aligned} M(\Delta w, e_t) \\ = (M_c(\Delta w_c, e_t), M_m(\Delta w_m, e_t), M_f(\Delta w_f, e_t)). \end{aligned} \quad (4)$$

To incorporate both text conditions and mask conditions into M_c and M_m , we modify the original modulation module by introducing a mask branch and a text branch to calculate corresponding scale and bias parameters $\alpha_m, \beta_m, \alpha_t$, and β_t . These parameters are then fused using a weight γ to obtain the final scale parameter α and bias parameter β . Finally, the input x is modulated using α and β as follows:

$$\begin{aligned} \alpha &= (1 - \gamma) * \alpha_m + \gamma * \alpha_t, \\ \beta &= (1 - \gamma) * \beta_m + \gamma * \beta_t, \\ x' &= (1 + \alpha) \frac{x - \mu_x}{\sigma_x} + \beta, \end{aligned} \quad (5)$$

where μ_x and σ_x denote the mean and standard deviation of x , respectively.

Simple Decoupling Strategy: Generating eyeglasses with diverse shapes and styles while preserving irrelevant regions presents a significant challenge. Our experimental observations suggest that this objective may compromise the diversity and realism of the generated eyeglasses. To address this issue, we propose a simple yet effective decoupling strategy comprising two operations: 1) We truncate the gradient flow from the disentangled mapper to the editing mapper, *i.e.*, the editing

mapper would not focus on preserving the irrelevant areas anymore. In this way, the editing mapper would achieve diverse eyeglasses styles along with significant modifications in the irrelevant areas. 2) Based on the results of the editing mapper, we then utilize the source image as supervision to reduce the modification in irrelevant areas and preserve the eyeglasses region meantime. That is, disentangled mapper mainly focuses on preserving the irrelevant areas without compromising the correctness and realism of the generated eyeglasses. In summary, with the decoupling strategy, the editing mapper mainly focuses on controlling the eyeglasses style while the disentangled mapper mainly focuses on preserving the irrelevant areas, without affecting each other.

D. Loss Function

In order to meet our objective of controlling the shape and style of eyeglasses in the manipulated image based on mask and text conditions, while preserving the irrelevant areas, we have devised several loss functions. The details are explained below.

Shape Consistency Loss: We propose a shape consistency loss that utilizes a face parser network [17] to guide our model in generating eyeglasses that are consistent with the given mask. Specifically, we first obtain the segmentation label S_{src} of the source image I_{src} using the face parser network P . Next, we combine S_{src} and the eyeglasses mask m to create the target segmentation label S_{tar} , which classifies pixels in the mask region as eyeglasses (excluding the eyes category) while leaving the others unchanged. The combination is defined as follows:

$$(S_{tar})_{ij} = \begin{cases} N_{glasses}, & \text{if } m_{ij} = 1 \& (S_{src})_{ij} \neq N_{eyes} \\ (S_{src})_{ij}, & \text{otherwise,} \end{cases} \quad (6)$$

where $N_{glasses}$ and N_{eyes} denote the category number of eyeglasses and eyes, respectively.

To ensure that the generated eyeglasses have the desired shape conditioned on m , we minimize the cross-entropy loss between S_{tar} and the predicted probability of the manipulated image I_{edit} . This allows our model to generate eyeglasses that are consistent with the given mask while preserving the irrelevant areas. The shape consistency loss is defined as follows:

$$\mathcal{L}_{sc} = CE(P(I_{edit}), S_{tar}), \quad (7)$$

where CE is cross-entropy loss.

Classification Loss: To avoid the undesirable phenomenon where GlassMapper relies on shortcuts that inconspicuous and mutilated eyeglasses may match the given mask and achieves a low shape consistency loss, we propose an eyeglasses classification loss. GlassMapper leverages this eyeglasses classifier¹ to distinguish between images with and without eyeglasses. The eyeglasses classification loss is expressed as:

$$\mathcal{L}_{cls} = Cg(I_{edit}), \quad (8)$$

where Cg denotes the eyeglasses classifier. Intuitively, if the classification score decreases, the present probability of

eyeglasses will increase, *i.e.*, eyeglasses in the manipulated image will be more fidelity and complete.

CLIP-NCE Loss: To perform eyeglasses style manipulation conditioned on the text description, we adopt the CLIP-based Noise Contrastive Estimation (CLIP-NCE) loss [13], which encourages the generated eyeglasses to be semantically similar to the input text description. It is defined as:

$$\mathcal{L}_{nce} = -\log \frac{e^{(Q \cdot K_T^+ / \tau)} + e^{(Q \cdot K_I^+ / \tau)}}{e^{(Q \cdot K_T^+ / \tau)} + e^{(Q \cdot K_I^+ / \tau)} + \sum_{K^-} (Q \cdot K^- / \tau)}, \quad (9)$$

where τ is the temperature and is set to 1.0. Q , K_T^+ , K_I^+ and K^- denote as query, text positive pairs, image positive pairs, and negative pairs, respectively.

Latent Loss and ID Loss: Similar to StyleCLIP [11], we adopt L2 distance to regularize the latent code and constrain the image domain; we also adopt cosine similarity to evaluate the facial feature similarity and preserve the identity information. The formulations are defined as follows:

$$\mathcal{L}_{norm} = \|w_{edit} - w_s\|_2, \quad (10)$$

$$\mathcal{L}_{id} = 1 - \cos(R(I_{edit}), R(I_{src})), \quad (11)$$

where R denotes ArcFace [56] network for face recognition.

Background Loss: To preserve the irrelevant areas, we directly compute pixel-wise mean square error between manipulated image I_{edit} and source image I_{src} , which is expressed as:

$$\mathcal{L}_{bg} = \|(I_{edit} - I_{src}) * (P_{ng}(I_{edit}) \cap (1 - m))\|_2, \quad (12)$$

where $P_{ng}()$ denotes non-eyeglasses areas mask.

Disentangled Loss: When editing the eyeglasses color, we observe a consequent change in cloth color. As the $W+$ space of StyleGAN exhibits strong semantic decoupling properties, we hypothesize that the entanglement issue may arise from the global guidance provided by CLIP, which may bind the color attribute to other objects, rather than eyeglasses. In other words, CLIP tends to identify an entangled editing direction in which clothing also conforms to color attributes, making it challenging to fully utilize the decoupling properties of $W+$ space. Therefore, as the RGB color space is not linearly correlated with human visual perception, we convert all the images from RGB color space to LAB [57] color space and define the disentangled loss as:

$$\mathcal{L}_{disentangle} = \lambda_g \|(I_{tar} - I_{edit}) * P_g(I_{edit})\|_2 + \lambda_c \|(I_{tar} - I_{src}) * P_c(I_{src})\|_2, \quad (13)$$

where $P_g()$ denotes eyeglasses area mask and $P_c()$ denotes cloth area mask. λ_g and λ_c are set to 4, 5 respectively. In this way, we achieve desired eyeglasses style in I_{tar} under the supervision of I_{edit} , and preserve the irrelevant area under the supervision of I_{src} .

E. Training Scheme

Intuitively, we can divide the whole task into two sub-tasks, one of which is to control the shape of eyeglasses based on the mask, and the other is to control the style of

¹https://github.com/apnkve/eyeglasses_on_photo

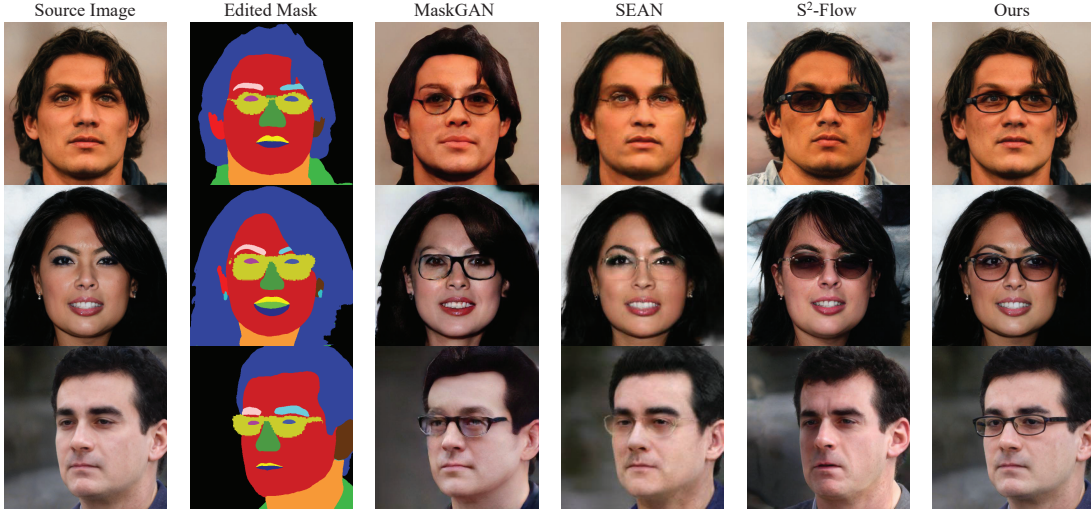


Fig. 4. Qualitative comparisons to semantic-based editing methods: MaskGAN [17], SEAN [58], S^2 -Flow [59]. Our approach successfully generates natural and high-fidelity eyeglasses consistent with the given semantic mask, along with a slight loss of identity information.

eyeglasses based on the text. As we observed that the training convergence speed of each sub-task is distinct, roughly 20 times the difference, it is challenging to train our framework end to end based on the mask and text simultaneously.

To handle the disparate training convergence rate of different modalities, we adopt a two-stage training approach. In the first stage (Stage-I), we train the editing mapper separately for each sub-task to enable preliminary control of the eyeglasses shape based on the mask and eyeglasses style based on text. In the second stage (Stage-II), we jointly train the editing mapper to simultaneously achieve all sub-tasks while introducing and learning the disentangled mapper to preserve the irrelevant areas. With this approach, we are able to control the eyeglasses shape and style based on the mask and text simultaneously, while also preserving the irrelevant areas.

Stage-I: Considering the distinct training convergence speed of each sub-task (*i.e.*, mask-guided eyeglasses shape manipulation and text-guided eyeglasses style manipulation), we separately train the editing mapper to achieve each sub-task. First, we focus on the sub-task of mask-guided eyeglasses manipulation, where we train the editing mapper to control the eyeglasses shape conditioned on the mask. Specifically, we set the weight γ to 0 and exclude the fine mapper, *i.e.*, only the mask encoder and mask branches in the course mapper and medium mapper are trainable. In this way, the objective function is defined as:

$$\mathcal{L} = \lambda_{sc}\mathcal{L}_{sc} + \lambda_{cls}\mathcal{L}_{cls} + \lambda_{norm}\mathcal{L}_{norm} + \lambda_{id}\mathcal{L}_{id} + \lambda_{bg}\mathcal{L}_{bg}, \quad (14)$$

where λ_{sc} , λ_{cls} , λ_{norm} , λ_{id} and λ_{bg} are set to 3, 0.03, 0.8, 0.1 and 2, respectively.

Later, we focus on the sub-task of text-guided eyeglasses manipulation, where we incorporate text conditions into the editing mapper to modify the eyeglasses style. Specifically, we freeze the parameters of the pre-trained mask encoder and mask branches and train all the text branches in the editing mapper. Moreover, we also set the weight γ to 0.5, which

means the mask conditions and text conditions contribute to the editing results equally. Finally, the objective function is:

$$\mathcal{L} = \lambda_{nce}\mathcal{L}_{nce} + \lambda_{norm}\mathcal{L}_{norm} + \lambda_{id}\mathcal{L}_{id}, \quad (15)$$

where λ_{nce} , λ_{norm} , λ_{id} , are set to 0.3, 0.8, and 0.2, respectively.

Stage-II: After Stage-I, the editing mapper has preliminary capabilities to achieve each sub-task separately, while performing poorly on the whole task. In other words, given a mask and text simultaneously, editing results would be overly modified based on the text, and also inconsistent with the mask. Therefore, we jointly train the editing mapper based on the mask and text simultaneously, *i.e.*, all the parameters in the editing mapper are trainable at this stage. To preserve the irrelevant areas, we also introduce and learn a disentangled mapper to predict more disentangled editing directions. Combined with the decoupling strategy, the editing mapper and the disentangled mapper would perform their duties independently of each other. Finally, the total objective function is:

$$\begin{aligned} \mathcal{L} = & \lambda_{nce}\mathcal{L}_{nce} + \lambda_{norm}\mathcal{L}_{norm} + \lambda_{id}\mathcal{L}_{id} \\ & + \lambda_{bg}\mathcal{L}_{bg} + \lambda_{sc}\mathcal{L}_{sc} + \lambda_{disentangle}\mathcal{L}_{disentangle}, \end{aligned} \quad (16)$$

where λ_{nce} , λ_{norm} , λ_{id} , λ_{bg} , λ_{sc} , and $\lambda_{disentangle}$ are set to 0.3, 0.8, 0.2, 5, 4, and 1, respectively.

IV. EXPERIMENTS

A. Implementation Details

Datasets: We use FFHQ dataset [23] for training and CelebA-HQ dataset [24] for evaluating. FFHQ consists of 70,000 face images acquired from Flickr and CelebA-HQ consists of 30,000 celebrity face images, both of which are at a resolution of 1024×1024 with considerable variations in appearances, poses, and backgrounds. Since we focus on the manipulation of eyeglasses, we split all the datasets based on the presence of eyeglasses. Specifically, we first utilize e4e [54] to obtain corresponding latent codes in the latent space



Fig. 5. Qualitative comparisons to text-based editing methods: StyleCLIP [11], PPE [25], CF-CLIP [13], DeltaEdit [44]. Each row demonstrates the editing results of different methods, and the text conditions are listed on the left side of each row. *Combined Image* denotes the combination of the source image and corresponding eyeglasses mask for better visualization. *Ours^{w/o mask}* denotes we ignore the effect of mask condition. Our approach successfully generated proper eyeglasses in all cases along with the least modification in irrelevant areas. It is noteworthy that comparison methods typically produce eyeglasses with identical shapes. In contrast, we can precisely control the shape of the eyeglasses using a binary mask.

of StyleGAN [23], [32]. Then we use an eyeglasses classifier² to classify the inversed images, where FFHQ/CelebA-HQ is divided into 12,698/1,341 images with eyeglasses and 51,598/25,489 images without eyeglasses. Notably, we filter out some images with inconspicuous eyeglasses whose classification scores are close to the threshold. Later, to obtain diverse eyeglasses masks, we utilize a face parser to segment all the images with eyeglasses and get 12,698/1,341 eyeglasses masks in FFHQ/CelebA-HQ. Finally, we construct aligned data pairs each of which is composed of an image without eyeglasses and an eyeglasses mask with the most similar pose³. In this way, we construct 12,698 data pairs in FFHQ as the training set and 1,341 data pairs in CelebA-HQ as the test set.

Training Details: We use an 18-layer StyleGAN2 [32] pretrained on FFHQ as our generator and the e4e [54] encoder pretrained on FFHQ as our inversion model. For CLIP [10] model, we utilize ViT-B/32 as a backbone to compute the similarity of image-text pairs, and the text encoder of CLIP is also used to obtain text embedding from the given text descriptions. For text input, we select seven common eyeglasses colors(*i.e.*,

red, blue, green, yellow, pink, orange, and purple) and two common eyeglasses styles(*i.e.*, metal glasses and sunglasses). As for training, Stage-I is trained for 150,000 iterations, among which we train the mask branches for 145,000 iterations with a base learning rate of 0.005 and train the text branches for 5,000 iterations with a base learning rate of 0.002. Stage-II is trained for 20,000 iterations with a base learning rate of 0.001. Throughout the training process, the batch size is set to 1. The optimizer is Adam [60] with β_1 and β_2 set to 0.9, 0.999, respectively.

Evaluation Metrics: To quantitatively evaluate the performance of our model, we use *Structure Similarity Index Measure* (SSIM) [26], *Peak Signal to Noise Ratio* (PSNR) [27], *Fréchet Inception Distances* (FID) [61], *Identity Discrepancy Scores* (IDS), *mean of class-wise Intersection over Union* (mIoU), and *Pixel Accuracy* (PA) as evaluation metrics: 1) SSIM and PSNR are calculated in the non-eyeglasses region between the source images and the editing results to quantify the capability of preserving irrelevant areas, using torchmetrics⁴. 2) FID calculates the distance between the feature vectors of the source images and the editing images, which is widely used to reflect the quantity and realism of the

²<https://drive.google.com/drive/folders/1MvYdWCBuMfnoYGptRH-AgKLbPTsIQIhL>

³Facial landmarks are identified by Dlib, and the facial image pose is computed based on a general 3D face model

⁴<https://github.com/Lightning-AI/metrics>

TABLE I

QUANTITATIVE COMPARISONS TO SEMANTIC-BASED EDITING METHODS. WE ACHIEVE BETTER RESULTS IN MOST CASES, DEMONSTRATING A STRIKING EDITING CAPABILITY OF PRESERVING IRRELEVANT AREAS AND GENERATING HIGH-FIDELITY EYEGLASSES CONSISTENT WITH THE GIVEN SEMANTIC MASK SIMULTANEOUSLY.

Method	SSIM(\uparrow)	PSNR(\uparrow)	IDS(\uparrow)	FID(\downarrow)	mIoU(\uparrow)	PA(\uparrow)
MaskGAN [17]	0.7086	20.6624	0.2823	39.44	0.6926	0.8985
SEAN [58]	0.7365	21.3615	0.4621	15.30	0.7087	0.9117
S^2 -Flow [59]	0.6824	16.5182	0.6057	21.81	0.6342	0.8878
Ours	0.8936	27.7014	0.7009	27.10	0.7741	0.9584

editing results. 3) IDS indicates identity similarity calculated by Curricularface [62]. 4) mIoU and PA are widely used in the semantic segmentation area, while in our experiments, we utilize them to reflect the consistency of the edited semantic mask and the editing results. We calculate all the evaluation metrics over our test split, *i.e.*, 1,341 real images in CelebA-HQ dataset [24].

B. Qualitative and Quantitative Comparison

Comparison to Semantic-based Editing Methods: To evaluate our capability of controlling the eyeglasses shape, we select three semantic-based image editing methods for comparison: MaskGAN [17], SEAN [58], and S^2 -Flow [59]. All the following comparison experiments are based on their pre-trained models.

The qualitative results are shown in Fig. 4. As illustrated in Fig. 4, our method demonstrates superior performance in terms of consistency in eyeglasses shape and preservation of identity information. MaskGAN [17] successfully generates eyeglasses consistent with the edited semantic mask, while the editing results are unnatural with a severe loss of identity. On the contrary, SEAN [58] better preserves the irrelevant areas and identity information while generating low-fidelity eyeglasses. Visually, S^2 -Flow [59] has a better trade-off between generating high-fidelity eyeglasses and preserving irrelevant areas. However, it fails to generate eyeglasses consistent with the given semantic mask in some cases. Benefiting from the shape consistency loss, we successfully generate natural and high-fidelity eyeglasses consistent with the given binary mask, along with a slight loss of identity information.

Table I presents the results of our quantitative comparison experiment to evaluate our capability of preserving irrelevant areas and generating high-fidelity eyeglasses, compared to other semantic-based editing methods. Compared with other semantic-based editing methods, we achieve a significant improvement in SSIM, PSNR, and IDS metrics, which demonstrates our capability of preserving irrelevant areas and identity information. We also get the best results on mIoU and PA metrics, demonstrating the extraordinary capacity to generate high-fidelity eyeglasses consistent with the given semantic mask. In terms of FID, we still achieve comparable results, indicating that the distribution of editing results is similar to the source images. In total, we demonstrate a striking editing capability of preserving irrelevant areas and generating high-fidelity eyeglasses simultaneously.



Fig. 6. Ablation analysis of \mathcal{L}_{cls} and \mathcal{L}_{sc} . *Combined Image* denotes the combination of the source image and corresponding eyeglasses mask for better visualization. By incorporating both the classification loss (\mathcal{L}_{cls}) and the shape consistency loss (\mathcal{L}_{sc}), we can generate eyeglasses that are more complete and realistic.

Comparison to Text-based Editing Methods: We compare our model to four state-of-the-art text-guided image manipulation methods: StyleCLIP [11], PPE [25], CF-CLIP [13], and DeltaEdit⁵ [44]. Since these compared methods do not involve mask conditions, we simply focus on the capabilities of modifying the eyeglasses style based on text conditions for a fair comparison, *i.e.*, we do not calculate mIoU and PA during quantitative comparison.

The qualitative results over CelebA-HQ dataset [24] are shown in Fig. 5, our method achieves more natural and realistic results while preserving the irrelevant areas to the greatest extent. StyleCLIP [11] successfully achieves most of the eyeglasses styles besides sunglasses, along with a significant modification on irrelevant areas, *e.g.*, hair, skin, and cloth. Focusing on disentangling editing, PPE [25] reduces changes in most of the irrelevant areas, while still failing in the sunglasses setting. CF-CLIP [13] achieves all the eyeglasses styles we demonstrated, but it may suffer from an excessive modification issue, *e.g.* the lens is also modified in the setting of blue glasses and green glasses. DeltaEdit [44], which is designed to perform arbitrary text-guided image manipulation, fails to produce satisfactory results in any of our experimental settings, even when the editing scale is increased. This illustrates the challenge of manipulating eyeglasses based solely on text prompts. Meanwhile, all the comparison methods fail to preserve the cloth region when modifying the eyeglasses color. Thanks to the disentangled mapper and the simple decoupling strategy, we successfully preserve the cloth region in most cases, regardless of whether we incorporate or ignore the spatial information. Moreover, since we control the shape and style of eyeglasses in a single model, we mitigate the excessive modification phenomenon by keeping the balance of each eyeglasses style.

In Table II, we give the quantitative comparison results of modifying eyeglasses styles. Notably, as observed in the

⁵In the comparison experiments, we multiply their editing scale since there are no significant alterations in the initial configuration.

TABLE II
QUANTITATIVE COMPARISONS TO TEXT-BASED EDITING METHODS. * DENOTES WE IGNORE THE CORRESPONDING RESULTS DUE TO THE FAILURE OF GENERATING DESIRED EYEGLASSES. IN MOST CASES, WE ACHIEVE SIGNIFICANT IMPROVEMENTS, INDICATING THE SUPERIOR CAPABILITY OF PRESERVING IRRELEVANT AREAS AND IDENTITY INFORMATION.

(a) Quantitative comparisons on SSIM and PSNR										
Attribute	SSIM(\uparrow)					PSNR(\uparrow)				
	SC [11]	PPE [25]	CF [13]	DE [44]	Ours	SC [11]	PPE [25]	CF [13]	DE [44]	Ours
Red Glasses	0.7527	0.8092	0.781	0.7551	0.8763	18.6167	20.5294	19.7347	18.2238	25.6752
Green Glasses	0.6809	0.7685	0.7706	0.7671	0.8726	15.9091	18.2201	18.5541	18.7533	25.2754
Blue Glasses	0.675	0.7998	0.7797	0.7438	0.885	15.0246	19.2803	18.9938	17.7292	26.5254
Yellow Glasses	0.7556	0.7913	0.7822	0.7623	0.8765	16.5762	18.5811	17.8985	18.6277	25.4507
Sunglasses	*	*	0.779	0.7955	0.8853	*	*	20.4889	20.0674	26.5156
Metal Glasses	0.7866	0.8688	0.7815	0.7723	0.8955	19.2745	24.6519	19.8303	19.3684	27.7088
Average	0.7302	0.8075	0.7790	0.7660	0.8819	17.0802	20.2526	19.2501	18.7950	26.1919

(b) Quantitative comparisons on IDS and FID										
Attribute	IDS(\uparrow)					FID(\downarrow)				
	SC [11]	PPE [25]	CF [13]	DE [44]	Ours	SC [11]	PPE [25]	CF [13]	DE [44]	Ours
Red Glasses	0.5348	0.57	0.5499	0.4931	0.6543	133.63	149.05	148.71	36.34	73.64
Green Glasses	0.5352	0.5788	0.5027	0.4814	0.6425	107.13	113.93	157.54	42.95	113.43
Blue Glasses	0.4964	0.5763	0.4956	0.4950	0.6703	100.15	95.29	149.75	41.33	58.8
Yellow Glasses	0.5403	0.5721	0.5617	0.4772	0.6573	137.44	159.48	122.06	45.92	111.52
Sunglasses	*	*	0.4777	0.3932	0.6169	*	*	213.34	69.82	120.78
Metal Glasses	0.522	0.7238	0.5299	0.4810	0.6998	32.28	20.63	37.9	57.55	24.77
Average	0.5257	0.5911	0.5196	0.4701	0.6569	102.13	107.68	138.22	48.98	94.55

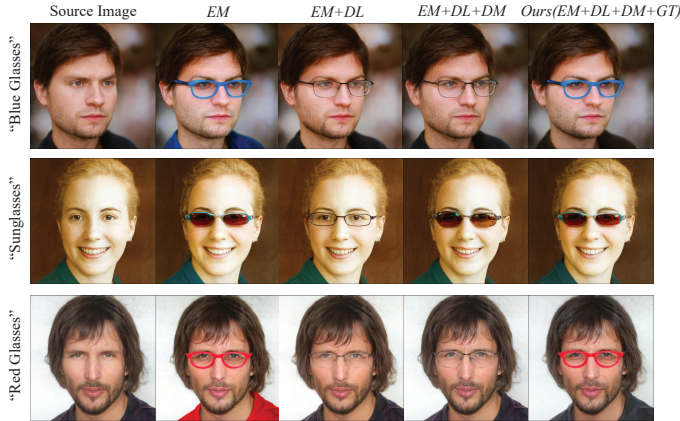


Fig. 7. Ablation analysis of the disentangled mapper and decoupling strategy. *EM*, *DL*, *DM*, and *GT* denote the editing mapper, disentangling loss, disentangled mapper, and gradient flow truncation, respectively. It indicates that both the disentangled mapper and decoupling strategy is necessary to preserve the irrelevant areas.

visual results, StyleCLIP [11] and PPE [25] fail to generate sunglasses, thus we ignore the corresponding quantitative results for a fair comparison. As can be seen, we achieve the best SSIM and PSNR scores in all the eyeglasses style settings, significantly greater than other comparison methods, which demonstrates our capability of preserving the irrelevant areas. Meanwhile, we also better preserve the identity information as we achieve better IDS scores in most cases besides the metal eyeglasses setting. In a word, we outperform the state of the arts by 9.21%, 29.32%, and 11.13% on SSIM, PSNR, and IDS on average. All the quantitative results are consistent with our visual comparison, *i.e.*, our approach can not only generate

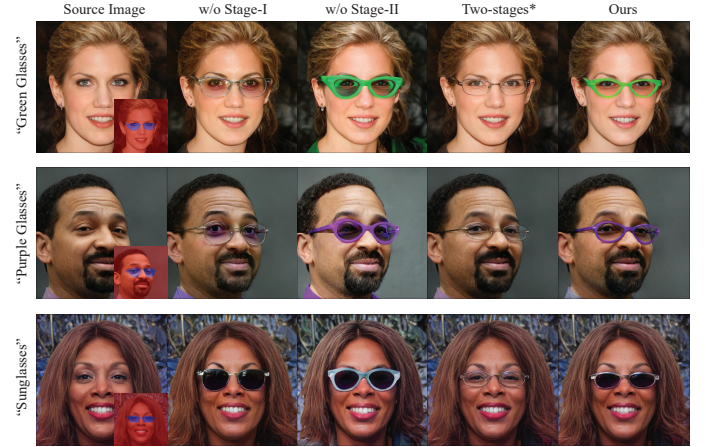


Fig. 8. Ablation analysis of the two-stage training scheme. *Two-stage** denotes we exchange the training orders in Stage-I. Only by using the two-stage training scheme, did we succeed to control the shape and style of the eyeglasses simultaneously.

natural and realistic eyeglasses in the editing results but also preserve the irrelevant areas to the greatest extent.

We found that DeltaEdit [44] achieves the best FID scores, but it fails to produce visually appealing results in all our experimental settings. This suggests that FID may not be an appropriate metric for evaluating the manipulation capability of these methods, which is consistent with the findings in [12].

In eyeglasses virtual try-on, the goal is to add eyeglasses to a face, which leads to a significant difference in distribution between the source images and the edited results, resulting in a higher FID score. DeltaEdit achieves a lower FID score at the cost of achieving the desired manipulation, which

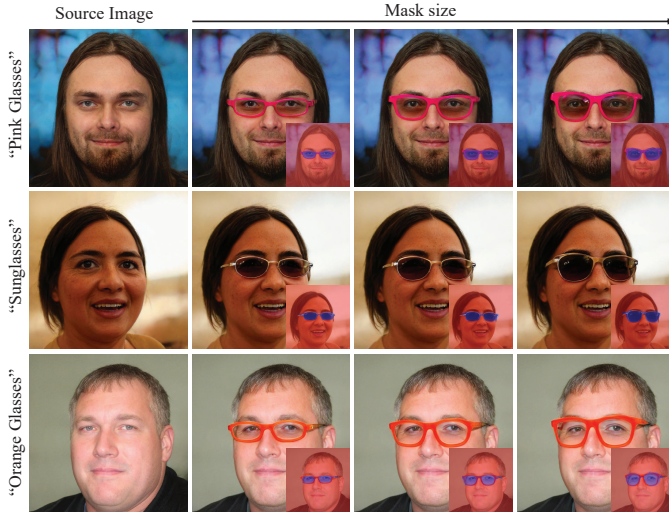


Fig. 9. Visual results based on diverse mask conditions. As the eyeglasses mask dilates sequentially, our framework succeeds to generate well-aligned eyeglasses, without changing the eyeglasses style by text.

is contrary to our primary objective. Compared with other methods that successfully achieve the desired manipulation, our approach also receives the lowest FID score, indicating that our generated images are more natural and realistic

C. Ablation Analysis

Importance of Shape Consistency Loss and Classification Loss: During our two-stage training process, we use several loss functions to control the generated eyeglasses and preserve the irrelevant areas. We employ widely-used loss functions such as \mathcal{L}_{nce} , \mathcal{L}_{id} , \mathcal{L}_{norm} , and \mathcal{L}_{bg} , which have proven their effectiveness in manipulating desired face attributes while keeping irrelevant regions unchanged. We introduce \mathcal{L}_{cls} and \mathcal{L}_{sc} to better control the shape and alignment of the eyeglasses. Visual examples in Fig. 6 demonstrate that using both \mathcal{L}_{cls} and \mathcal{L}_{sc} generates more complete and realistic eyeglasses that are well-aligned with the given mask. Dropping either of these loss functions leads to noticeable issues, such as mutilated eyeglasses or misaligned eyeglasses. Our results confirm the effectiveness of using \mathcal{L}_{cls} to generate more fidelity and realistic results while avoiding shortcuts that may lead to inconspicuous or mutilated eyeglasses matching the given mask. Additionally, utilizing \mathcal{L}_{sc} is crucial in producing well-aligned eyeglasses with the preferred spatial configuration, preventing the occurrence of uniform eyeglasses with identical forms.

Impact of Disentangled Mapper and Decoupling Strategy: To better preserve irrelevant areas, we propose a disentangled mapper and a simple decoupling strategy, *i.e.*, truncate the gradient flow computed by the disentangling loss. Therefore, we compare several variants to verify the effect of our disentangled mapper and decoupling strategy. As shown in Fig. 7, solely with the editing mapper, we successfully achieve desired eyeglasses style, but there present significant modifications in the irrelevant areas, especially the cloth region. When including the disentangling loss, we

better preserve the irrelevant areas, while failing in generating desired eyeglasses, indicating that the disentangling loss may impair the capability of the editing mapper to generate desired eyeglasses. Moreover, when including both disentangling loss and disentangled mapper, we still suffer from the same issue above, while the difference is that we succeed to generate sunglasses thanks to the disentangled mapper. Combining the disentangled mapper and disentangling loss with gradient flow truncation, our approach both achieves diverse eyeglasses styles and preserves the irrelevant areas well. In other words, by truncating the gradient flow, the editing mapper mainly focuses on controlling the eyeglasses style while the disentangled mapper mainly focuses on preserving the irrelevant areas, without affecting each other.

Two-Stage Training Scheme: In Fig. 8, we compare the editing results using different training schemes. First, we exclude Stage-I, where we jointly train our model based on the mask and text conditions simultaneously. In this setting, we only succeed in generating sunglasses, and the eyeglasses shapes are not aligned with the mask. Second, we exclude Stage-II, where we do not jointly train our model after the preliminary training of Stage-I. Although all the editing results are well-aligned with the text descriptions, the eyeglasses shapes are different from the given mask, indicating a loss of the ability to control the eyeglasses shape. In conclusion, these phenomena prove the necessity of each stage in the training scheme.

Moreover, to evaluate the influence of training orders in Stage-I, we adopt another two-stage training scheme. We first train our model based on the text conditions and then based on the mask conditions. As can be seen, when we exchange the training orders in Stage-I, the eyeglasses shape is well-aligned with the mask, while the eyeglasses style is virtually unaffected by the text. That is, training our model based on the mask conditions will severely affect the ability to control the eyeglasses style. Therefore, it is necessary to keep the original training orders in Stage-I to avoid the loss of the ability to change diverse eyeglasses styles based on the text.

Decoupling Properties between Different Conditions: Though we achieve controllable eyeglasses manipulation based on different conditions, is the model really controlling the eyeglasses shape and style based on the mask and text conditions separately as we hoped, without affecting each other? To explore how these two conditions contribute to the modification process, we conduct two experiments that preserve one condition while changing the other.

First, we preserve the text description while changing the size of eyeglasses mask. As shown in Fig. 9, our framework success to generate natural and realistic eyeglasses of diverse shapes under different head poses, without changing the eyeglasses style. Second, we preserve the mask condition while changing the text descriptions. Specifically, we choose four basic colors(*i.e.*, blue, red, green, and yellow) and two common styles(*i.e.*, sunglasses, metal glasses). As demonstrated in Fig. 10, we successfully achieve desired eyeglasses style which is well-aligned with different text descriptions, and the eyeglasses shape is still consistent with the given mask.

These results indicate that the mask conditions and text con-

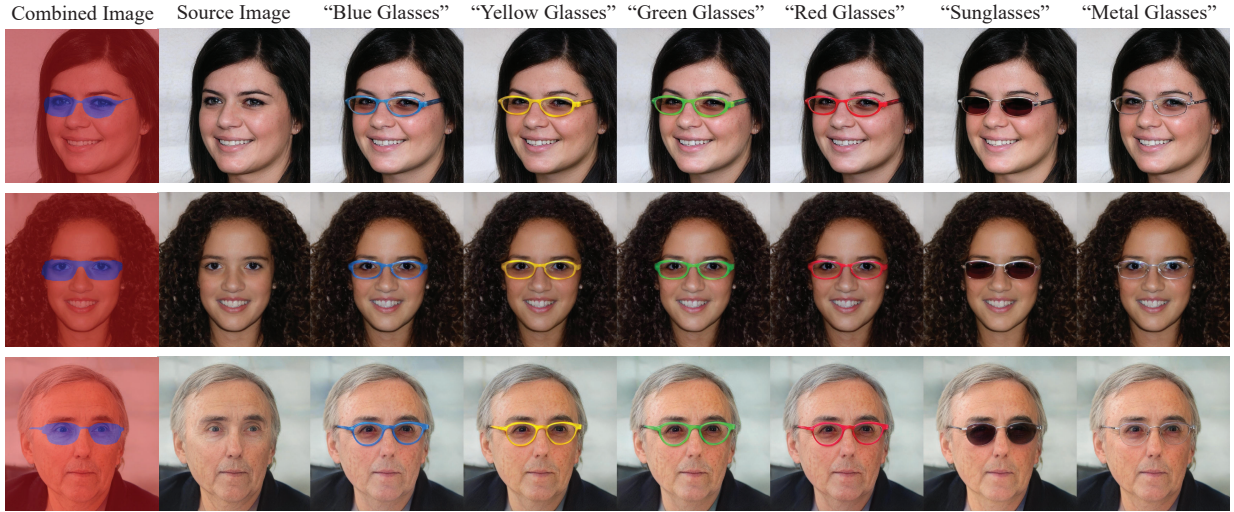


Fig. 10. Visual results based on diverse text conditions. *Combined Image* denotes the combination of the source image and corresponding eyeglasses mask for better visualization. As we change the text conditions, generated eyeglasses are well-aligned with the corresponding text, preserving the shape determined by the given mask.

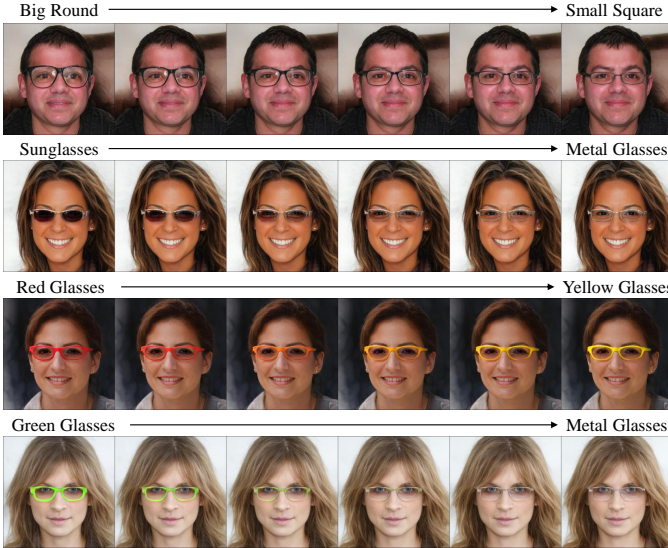


Fig. 11. Interpolation results. The first row demonstrates the interpolation results between different eyeglasses shapes, and the rest rows show the interpolation results between different eyeglasses styles. All the intermediate results are natural and realistic, with few artifacts.

ditions control the eyeglasses in a decoupling way, meaning that the mask conditions would not influence the eyeglasses style, and text conditions would not influence the eyeglasses shape. This allows for more controllable manipulation of the eyeglasses, such as modifying the eyeglasses shape and style individually or simultaneously.

Interpolation Results: To demonstrate the smoothness of the editing, we conduct two kinds of interpolation experiments, *i.e.*, mask interpolation and text interpolation. In detail, given two edited latent codes w_a and w_b , we linearly combine them to get an intermediate latent code $w_{inter} = \eta w_a + (1 - \eta)w_b$, where the weight η rises from 0 to 1 with an interval of 0.2.

As shown in Fig. 11, we interpolate the editing results based

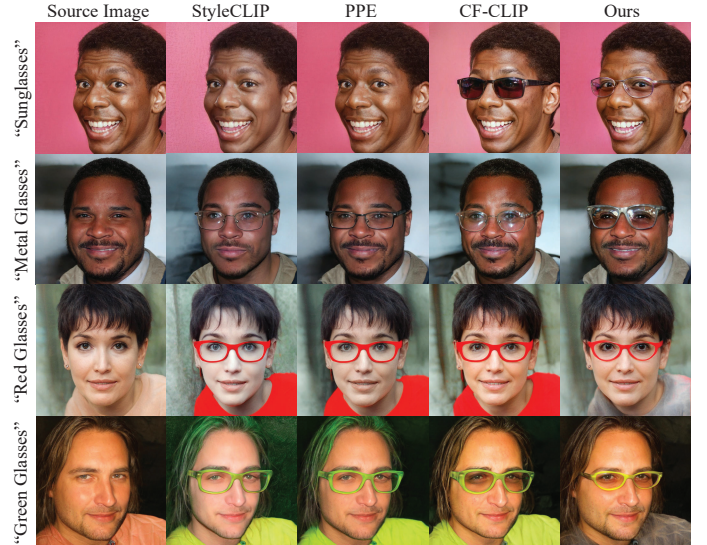


Fig. 12. Failure examples. The first two rows show the failed examples of generating sunglasses and metal glasses, and the last two rows show the failed examples of preserving the irrelevant areas. Please note that we do not provide examples of DeltaEdit [44], as it fails in most cases.

on different masks and text, respectively. In the first row, we interpolate between two editing results, one with big round glasses and the other with small square glasses, resulting in a series of intermediate images. While in the last three rows, we get the intermediate images by interpolating the editing results with different eyeglasses styles. Visually, whether we interpolate eyeglasses shapes or styles, the intermediate results are realistic and natural with fewer artifacts, proving the smoothness of the learned editing directions.

D. Failure Examples

We present some failure examples of our approach in Fig. 12. The first two rows show the failures in generating sun-

glasses and metal glasses, *i.e.*, the generated eyeglasses do not conform to sunglasses or metal glasses. Intuitively, different eyeglasses styles correspond to different editing operations, *e.g.*, changing eyeglasses color tends to color and thicken the frame for better visuality, while generating metal glasses and sunglasses tends to thin the frame and darken the lens, respectively. Since we achieve diverse eyeglasses styles with one model, it is difficult to find an optimal balance between the contradictory goals of different eyeglasses styles. Therefore, the capability of generating metal glasses and sunglasses is slightly worse, resulting in some failure examples. The last two rows show the failures in preserving the irrelevant areas. As can be seen, when there is a large range of solid color cloth in the source image, our approach seems to overly preserve the cloth areas, resulting in the loss of original color. As observed in the dataset, cloth does not present in all images, and the cloth area is also of different sizes and styles. Therefore, our approach is difficult to handle the uncommon samples in the dataset, *e.g.*, images with a large range of solid cloth, failing in preventing the modification of irrelevant areas, especially cloth regions. It is noteworthy that the majority of comparison methods exhibit similar failures, suggesting that these cases present a significant challenge for all approaches.

V. CONCLUSION

Focusing on eyeglasses virtual try-on, we propose a Text-guided Eyeglasses Manipulation method to control the eyeglasses shape and style based on the mask and text, which is intuitive and effective. Thanks to the new modulation module and two-stage training scheme, the mask conditions and text conditions control the eyeglasses simultaneously in a decoupling way, which is a more flexible and controllable interaction way. Furthermore, by utilizing the simple but effective decoupling strategy, we preserve the irrelevant areas to a great extent, resulting in better local editing. Quantitative and Qualitative Comparison and ablation analysis demonstrate the superiority of our approach to achieve diverse and realistic eyeglasses and preserve the irrelevant areas in the editing results.

Future research may focus on streamlining the training process, which currently necessitates separate training for each modality followed by joint training. Another potential avenue for improvement is the generalization to more challenging cases, such as highly regular eyeglasses shapes or unusual eyeglasses styles. The collection of additional extreme eyeglasses masks and unusual eyeglasses prompts may provide a viable solution.

REFERENCES

- [1] M. Milanova and F. Aldaeif, "Markerless 3d virtual glasses try-on system," in *New Approaches for Multidimensional Signal Processing*, 2021, pp. 99–111.
- [2] Z. Feng, F. Jiang, and R. Shen, "Virtual glasses try-on based on large pose estimation," *Procedia Computer Science*, vol. 131, pp. 226–233, 2018.
- [3] D. Marelli, S. Bianco, and G. Ciocca, "Faithful fit, markerless, 3d eyeglasses virtual try-on," in *International Conference on Pattern Recognition*, 2021, pp. 460–471.
- [4] —, "A web application for glasses virtual try-on in 3d space," in *2019 IEEE 23rd International Symposium on Consumer Technologies*, 2019, pp. 299–303.
- [5] —, "Designing an ai-based virtual try-on web application," *Sensors*, vol. 22, no. 10, p. 3832, 2022.
- [6] X. Li, S. Zhang, J. Hu, L. Cao, X. Hong, X. Mao, F. Huang, Y. Wu, and R. Ji, "Image-to-image translation via hierarchical style disentanglement," in *Proceedings of the IEEE/CVF Conference on Computer Vision and Pattern Recognition*, 2021, pp. 8639–8648.
- [7] Y. Shen, J. Gu, X. Tang, and B. Zhong, "Interpreting the latent space of gans for semantic face editing," in *Proceedings of the IEEE/CVF Conference on Computer Vision and Pattern Recognition*, 2020, pp. 9243–9252.
- [8] E. Härkönen, A. Hertzmann, J. Lehtinen, and S. Paris, "Ganspace: Discovering interpretable gan controls," *Advances in Neural Information Processing Systems*, vol. 33, pp. 9841–9850, 2020.
- [9] I. J. Goodfellow, J. Pouget-Abadie, M. Mirza, B. Xu, D. Warde-Farley, S. Ozair, A. C. Courville, and Y. Bengio, "Generative adversarial nets," in *Advances in Neural Information Processing Systems*, 2014, pp. 2672–2680.
- [10] A. Radford, J. W. Kim, C. Hallacy, A. Ramesh, G. Goh, S. Agarwal, G. Sastry, A. Askell, P. Mishkin, J. Clark *et al.*, "Learning transferable visual models from natural language supervision," in *International Conference on Machine Learning*, 2021, pp. 8748–8763.
- [11] O. Patashnik, Z. Wu, E. Shechtman, D. Cohen-Or, and D. Lischinski, "Styleclip: Text-driven manipulation of stylegan imagery," in *Proceedings of the IEEE/CVF International Conference on Computer Vision*, 2021, pp. 2085–2094.
- [12] T. Wei, D. Chen, W. Zhou, J. Liao, Z. Tan, L. Yuan, W. Zhang, and N. Yu, "Hairclip: Design your hair by text and reference image," in *Proceedings of the IEEE/CVF Conference on Computer Vision and Pattern Recognition*, 2022, pp. 18 072–18 081.
- [13] Y. Yu, F. Zhan, R. Wu, J. Zhang, S. Lu, M. Cui, X. Xie, X.-S. Hua, and C. Miao, "Towards counterfactual image manipulation via clip," in *Proceedings of the 30th ACM International Conference on Multimedia*, 2022, pp. 3637–3645.
- [14] R. Gal, O. Patashnik, H. Maron, A. H. Bermano, G. Chechik, and D. Cohen-Or, "Stylegan-nada: Clip-guided domain adaptation of image generators," *ACM Transactions on Graphics*, vol. 41, no. 4, pp. 1–13, 2022.
- [15] T. Zhao, T. Zhang, M. Zhu, H. Shen, K. Lee, X. Lu, and J. Yin, "Vi-checklist: Evaluating pre-trained vision-language models with objects, attributes and relations," *arXiv preprint arXiv:2207.00221*, 2022.
- [16] E. Zakharov, A. Ivakhnenko, A. Shysheya, and V. Lempitsky, "Fast bi-layer neural synthesis of one-shot realistic head avatars," in *European Conference on Computer Vision*, 2020, pp. 524–540.
- [17] C.-H. Lee, Z. Liu, L. Wu, and P. Luo, "Maskgan: Towards diverse and interactive facial image manipulation," in *Proceedings of the IEEE/CVF Conference on Computer Vision and Pattern Recognition*, 2020, pp. 5549–5558.
- [18] D. Bau, A. Andonian, A. Cui, Y. Park, A. Jahanian, A. Oliva, and A. Torralba, "Paint by word," *arXiv preprint arXiv:2103.10951*, 2021.
- [19] A. Bulat and G. Tzimiropoulos, "How far are we from solving the 2d & 3d face alignment problem?(and a dataset of 230,000 3d facial landmarks)," in *Proceedings of the IEEE International Conference on Computer Vision*, 2017, pp. 1021–1030.
- [20] J. Xia, W. Qu, W. Huang, J. Zhang, X. Wang, and M. Xu, "Sparse local patch transformer for robust face alignment and landmarks inherent relation learning," in *Proceedings of the IEEE/CVF Conference on Computer Vision and Pattern Recognition*, 2022, pp. 4052–4061.
- [21] G. Te, W. Hu, Y. Liu, H. Shi, and T. Mei, "Agrnet: Adaptive graph representation learning and reasoning for face parsing," *IEEE Transactions on Image Processing*, vol. 30, pp. 8236–8250, 2021.
- [22] Y. Zheng, H. Yang, T. Zhang, J. Bao, D. Chen, Y. Huang, L. Yuan, D. Chen, M. Zeng, and F. Wen, "General facial representation learning in a visual-linguistic manner," in *Proceedings of the IEEE/CVF Conference on Computer Vision and Pattern Recognition*, 2022, pp. 18 697–18 709.
- [23] T. Karras, S. Laine, and T. Aila, "A style-based generator architecture for generative adversarial networks," in *Proceedings of the IEEE/CVF Conference on Computer Vision and Pattern Recognition*, 2019, pp. 4401–4410.
- [24] T. Karras, T. Aila, S. Laine, and J. Lehtinen, "Progressive growing of gans for improved quality, stability, and variation," in *6th International Conference on Learning Representations*, 2018.
- [25] Z. Xu, T. Lin, H. Tang, F. Li, D. He, N. Sebe, R. Timofte, L. Van Gool, and E. Ding, "Predict, prevent, and evaluate: Disentangled text-driven image manipulation empowered by pre-trained vision-language model,"

- in *Proceedings of the IEEE/CVF Conference on Computer Vision and Pattern Recognition*, 2022, pp. 18 229–18 238.
- [26] Z. Wang, A. C. Bovik, H. R. Sheikh, and E. P. Simoncelli, “Image quality assessment: from error visibility to structural similarity,” *IEEE Transactions on Image Processing*, vol. 13, no. 4, pp. 600–612, 2004.
- [27] J. Korhonen and J. You, “Peak signal-to-noise ratio revisited: Is simple beautiful?” in *2012 Fourth International Workshop on Quality of Multimedia Experience*, 2012, pp. 37–38.
- [28] B. Hu, Z. Zheng, P. Liu, W. Yang, and M. Ren, “Unsupervised eyeglasses removal in the wild,” *IEEE Transactions on Cybernetics*, vol. 51, no. 9, pp. 4373–4385, 2020.
- [29] Y.-H. Lee and S.-H. Lai, “Byeglassesgan: Identity preserving eyeglasses removal for face images,” in *European Conference on Computer Vision*, 2020, pp. 243–258.
- [30] Y. Shen and B. Zhou, “Closed-form factorization of latent semantics in gans,” in *Proceedings of the IEEE/CVF Conference on Computer Vision and Pattern Recognition*, 2021, pp. 1532–1540.
- [31] Z. He, W. Zuo, M. Kan, S. Shan, and X. Chen, “Attgan: Facial attribute editing by only changing what you want,” *IEEE Transactions on Image Processing*, vol. 28, no. 11, pp. 5464–5478, 2019.
- [32] T. Karras, S. Laine, M. Aittala, J. Hellsten, J. Lehtinen, and T. Aila, “Analyzing and improving the image quality of stylegan,” in *Proceedings of the IEEE/CVF Conference on Computer Vision and Pattern Recognition*, 2020, pp. 8110–8119.
- [33] R. Plesh, P. Peer, and V. Štruc, “Glassesgan: Eyewear personalization using synthetic appearance discovery and targeted subspace modeling,” *arXiv preprint arXiv:2210.14145*, 2022.
- [34] J. Huang, L. Jing, Z. Tan, and S. Kwong, “Multi-density sketch-to-image translation network,” *IEEE Transactions on Multimedia*, vol. 24, pp. 4002–4015, 2022.
- [35] X. Hou, X. Zhang, Y. Li, and L. Shen, “Textface: Text-to-style mapping based face generation and manipulation,” *IEEE Transactions on Multimedia*, pp. 1–1, 2022.
- [36] L. Liang and X. Zhang, “Adaptive label propagation for facial appearance transfer,” *IEEE Transactions on Multimedia*, vol. 21, no. 12, pp. 3068–3082, 2019.
- [37] S. Liu, R. Bao, D. Zhu, S. Huang, Q. Yan, L. Lin, and C. Dong, “Fine-grained face editing via personalized spatial-aware affine modulation,” *IEEE Transactions on Multimedia*, pp. 1–1, 2022.
- [38] Y. Liu, Y. Chen, L. Bao, N. Sebe, B. Lepri, and M. De Nadai, “Isf-gan: An implicit style function for high resolution image-to-image translation,” *IEEE Transactions on Multimedia*, pp. 1–1, 2022.
- [39] R. Paiss, H. Chefer, and L. Wolf, “No token left behind: Explainability-aided image classification and generation,” in *European Conference on Computer Vision*, 2022, pp. 334–350.
- [40] X. Hou, L. Shen, O. Patashnik, D. Cohen-Or, and H. Huang, “Feat: Face editing with attention,” *arXiv preprint arXiv:2202.02713*, 2022.
- [41] X. Liu, C. Gong, L. Wu, S. Zhang, H. Su, and Q. Liu, “Fusedream: Training-free text-to-image generation with improved clip+gan space optimization,” *arXiv preprint arXiv:2112.01573*, 2021.
- [42] J. Sun, Q. Deng, Q. Li, M. Sun, M. Ren, and Z. Sun, “Anyface: Free-style text-to-face synthesis and manipulation,” in *Proceedings of the IEEE/CVF Conference on Computer Vision and Pattern Recognition*, 2022, pp. 18 687–18 696.
- [43] W. Zheng, Q. Li, X. Guo, P. Wan, and Z. Wang, “Bridging clip and stylegan through latent alignment for image editing,” *arXiv preprint arXiv:2210.04506*, 2022.
- [44] Y. Lyu, T. Lin, F. Li, D. He, J. Dong, and T. Tan, “Deltaedit: Exploring text-free training for text-driven image manipulation,” *arXiv preprint arXiv:2303.06285*, 2023.
- [45] H. Wang, G. Lin, A. G. del Molino, A. Wang, Z. Yuan, C. Miao, and J. Feng, “Maniclip: Multi-attribute face manipulation from text,” *arXiv preprint arXiv:2210.00445*, 2022.
- [46] G. Kim, T. Kwon, and J. C. Ye, “Diffusionclip: Text-guided diffusion models for robust image manipulation,” in *Proceedings of the IEEE/CVF Conference on Computer Vision and Pattern Recognition*, 2022, pp. 2426–2435.
- [47] P. Chandramouli and K. V. Gandikota, “Ldedit: Towards generalized text guided image manipulation via latent diffusion models,” in *33rd British Machine Vision Conference*, 2022.
- [48] O. Avrahami, D. Lischinski, and O. Fried, “Blended diffusion for text-driven editing of natural images,” in *Proceedings of the IEEE/CVF Conference on Computer Vision and Pattern Recognition*, 2022, pp. 18 208–18 218.
- [49] J. Ho, A. Jain, and P. Abbeel, “Denoising diffusion probabilistic models,” *Advances in Neural Information Processing Systems*, vol. 33, pp. 6840–6851, 2020.
- [50] J. Song, C. Meng, and S. Ermon, “Denoising diffusion implicit models,” in *9th International Conference on Learning Representations*, 2021.
- [51] R. Rombach, A. Blattmann, D. Lorenz, P. Esser, and B. Ommer, “High-resolution image synthesis with latent diffusion models,” in *Proceedings of the IEEE/CVF Conference on Computer Vision and Pattern Recognition*, 2022, pp. 10 674–10 685.
- [52] Z. Wu, D. Lischinski, and E. Shechtman, “Stylespace analysis: Disentangled controls for stylegan image generation,” in *Proceedings of the IEEE/CVF Conference on Computer Vision and Pattern Recognition*, 2021, pp. 12 863–12 872.
- [53] R. Abdal, Y. Qin, and P. Wonka, “Image2stylegan: How to embed images into the stylegan latent space?” in *2019 IEEE/CVF International Conference on Computer Vision*, 2019, pp. 4431–4440.
- [54] O. Tov, Y. Alaluf, Y. Nitzan, O. Patashnik, and D. Cohen-Or, “Designing an encoder for stylegan image manipulation,” *ACM Transactions on Graphics*, vol. 40, no. 4, pp. 1–14, 2021.
- [55] W. Xia, Y. Yang, J.-H. Xue, and B. Wu, “Tedigan: Text-guided diverse face image generation and manipulation,” in *Proceedings of the IEEE/CVF Conference on Computer Vision and Pattern Recognition*, 2021, pp. 2256–2265.
- [56] J. Deng, J. Guo, N. Xue, and S. Zafeiriou, “Arcface: Additive angular margin loss for deep face recognition,” in *Proceedings of the IEEE/CVF Conference on Computer Vision and Pattern Recognition*, 2019, pp. 4690–4699.
- [57] T. Smith and J. Guild, “The cie colorimetric standards and their use,” *Transactions of the optical society*, vol. 33, no. 3, p. 73, 1931.
- [58] P. Zhu, R. Abdal, Y. Qin, and P. Wonka, “Sean: Image synthesis with semantic region-adaptive normalization,” in *Proceedings of the IEEE/CVF Conference on Computer Vision and Pattern Recognition*, 2020, pp. 5104–5113.
- [59] K. Singh, S. Schaub-Meyer, and S. Roth, “ $\mathcal{S}^2\mathcal{F}$ -flow: Joint semantic and style editing of facial images,” in *33rd British Machine Vision Conference 2022*, 2022, p. 821.
- [60] D. P. Kingma and J. Ba, “Adam: A method for stochastic optimization,” in *3rd International Conference on Learning Representations*, 2015.
- [61] M. Heusel, H. Ramsauer, T. Unterthiner, B. Nessler, and S. Hochreiter, “Gans trained by a two time-scale update rule converge to a local nash equilibrium,” *Advances in Neural Information Processing Systems*, vol. 30, pp. 6626–6637, 2017.
- [62] Y. Huang, Y. Wang, Y. Tai, X. Liu, P. Shen, S. Li, J. Li, and F. Huang, “Curricularface: adaptive curriculum learning loss for deep face recognition,” in *proceedings of the IEEE/CVF Conference on Computer Vision and Pattern Recognition*, 2020, pp. 5901–5910.